HHS Public Access

Author manuscript

Matrix Biol. Author manuscript; available in PMC 2017 May 01.

Published in final edited form as:

Matrix Biol. 2016 ; 52-54: 246–259. doi:10.1016/j.matbio.2016.01.003.

Accelerated enamel mineralization in *Dspp* mutant mice

Kostas Verdelis[a,b,c,d], **Heather L. Szabo-Rogers**[a,b,e], **Yang Xu**[a], **Rong Chong**[a], **Ryan Kang**[a], **Brian J. Cusack**[a], **Priyam Jani**[f], **Adele L. Boskey**[d], **Chunlin Qin**[f], and **Elia Beniash**[a,b,g]

[a] Center for Craniofacial Regeneration, Department of Oral Biology, School of Dental Medicine, University of Pittsburgh, PA 15261, United States

[b] McGowan Institute for Regenerative Medicine, Pittsburgh, PA 15261F, United States

[c] Department of Endodontics, School of Dental Medicine, University of Pittsburgh, PA 15261, United States

[d] Mineralized Tissues Laboratory, Hospital for Special Surgery, New York, NY 10021, United States

[e] Department of Developmental Biology, School of Medicine, University of Pittsburgh, PA 15201, United States

[f] Department of Biomedical Sciences and Center for Craniofacial Research and Diagnosis, Texas A&M University Baylor College of Dentistry, Dallas, TX 75246, United States

[g] Department of Bioengineering, Swanson School of Engineering, University of Pittsburgh, Pittsburgh, PA 15216, United States

Abstract

Dentin sialophosphoprotein (DSPP) is one of the major non-collagenous proteins present in dentin, cementum and alveolar bone; it is also transiently expressed by ameloblasts. In humans many mutations have been found in DSPP and are associated with two autosomal-dominant genetic diseases — dentinogenesis imperfecta II (DGI-II) and dentin dysplasia (DD). Both disorders result in the development of hypomineralized and mechanically compromised teeth. The erupted mature molars of *Dspp*$^{-/-}$ mice have a severe hypomineralized dentin phenotype. Since dentin and enamel formations are interdependent, we decided to investigate the process of enamel onset mineralization in young *Dspp*$^{-/-}$ animals. We focused our analysis on the constantly erupting mouse incisor, to capture all of the stages of odontogenesis in one tooth, and the unerupted first molars. Using high-resolution microCT, we revealed that the onset of enamel matrix deposition occurs closer to the cervical loop and both secretion and maturation of enamel are accelerated in *Dspp*$^{-/-}$ incisors compared to the *Dspp*$^{+/-}$ control. Importantly, these differences did not translate into major phenotypic differences in mature enamel in terms of the structural organization, mineral density or hardness. The only observable difference was the reduction in thickness of the outer enamel layer, while the total enamel thickness remained unchanged. We also observed a

Correspondence to Elia Beniash : University of Pittsburgh School of Dental Medicine, Swanson School of Engineering, McGowan Institute for Regenerative Medicine, 505 SALKP, 335 Sutherland Dr., Pittsburgh, 15213 PA, USA. Tel.: (1) 412 648 0108. ; Email: ebeniash@pitt.edu.

Appendix A. Supplementary data

Supplementary data to this article can be found online at http://dx.doi.org/10.1016/j.matbio.2016.01.003.

compromised dentin-enamel junction, leading to delamination between the dentin and enamel layers. The odontoblast processes were widened and lacked branching near the DEJ. Finally, for the first time we demonstrate expression of *Dspp* mRNA in secretory ameloblasts. In summary, our data show that DSPP is important for normal mineralization of both dentin and enamel.

Keywords

Odontogenesis; Dentin sialophosphoprotein; Dentin; Enamel; Dentino-enamel junction

Introduction

Tooth is an ectomesenchymal organ which develops via a series of reiterative signaling interactions between cells of oral epithelium and ectomesenchyme [1]. After initial steps of odontogenesis, determining tooth position and shape, the differentiation and biomineralization of the dentin and enamel tissues begin [2]. Enamel is formed by specialized ectodermal cells – ameloblasts, while dentin is produced by neural crest cells – odontoblasts. Dentin and enamel both form via appositional growth. At the beginning of matrix deposition, the ameloblasts and odontoblasts line up along a basal lamina which outlines the location of the future dentino-enamel junction (DEJ). Initially odonto-blasts start to secrete dentin collagenous matrix and retract from the DEJ leaving behind long cell processes residing in dentinal tubules. The cellular processes penetrate the whole thickness of the tissue from the DEJ to the pulp cavity. Once the mantle dentin (the layer of dentin adjacent to DEJ) starts to mineralize ameloblasts degrade the basal lamina and begin to deposit enamel, which marks the beginning of the secretory stage of amelogenesis [3–5]. The initial enamel is a network of nanocrystals embedded in a protein hydrogel. It contains about 10% mineral by volume [6]. Once the full thickness of enamel is deposited enamel maturation begins, involving removal of the organic matrix and mineralization via thickening of preexisting nascent crystallites [5].

In the mouse, the first tooth to erupt is the incisor, followed by 1st, 2nd and 3rd molars, which erupt sequentially during the 1st month after birth. The continuously developing unicuspid mouse incisor is an excellent model for biomineralization. The mandibular incisor has simple cylindrical morphology, which makes it more amenable to structural and compositional analyses, especially since the successive stages of amelogenesis can be seen in one sagittal section of the mandibular incisor (Fig. 1A,B). Although mouse molars are more similar to human teeth both in terms of their anatomy and the fact that they do not grow after eruption, the complex morphology of the multi-cusped molar does not permit the study of the successive stages of enamel formation.

Biomineralization of dentin and enamel is a process tightly controlled by matrix macromolecules which are involved in regulation of mineral nucleation, shape and organization of mineral particles. Dentin sialophosphoprotein (DSPP) is the major non-collagenous protein of dentin [7]. DSPP belongs to the SIBLING (Small Integrin-binding ligand, N-linked Glycoprotein) family of proteins and is primarily associated with mineralized tissues [8,9]. DSPP expressions (protein and mRNA) were found in dentin [10–

13], periodontium, alveolar bone and condylar cartilage [14–16]. It is also a transiently expressed in presecretory polarized ameloblasts prior to dentin deposition [17–20]. Upon secretion, DSPP is cleaved into two proteins — dentin sialoprotein (DSP) and dentin phosphoprotein (DPP) [21,22]. In porcine teeth a third proteolytic cleavage product, dentin glycoprotein (DGP), which is found N-terminal to DPP and considered to be a part of DSP [22–25] have been identified. Cleavage of DSPP is required for the proper dentin formation [26]. In humans mutations in *DSPP* cause dentinogenesis imperfecta (DGI) and dentin dysplasia (DD) [12]. Additional mutations in *DSPP* have been reported in two families with hypoplastic enamel [27]. DSP and DPP are extensively post-translationally modified [11].

DSP is a proteoglycan containing a single chondroitin-6-sulfate chain and several N-acetyl-neuraminic acids [28–31], while DPP is the most highly phosphorylated protein and contains ~200 phosphoserine residues [32]. Porcine DGP possesses one glycosylated asparagine and 4 phosphorylated serine residues [23]. DPP specifically binds to collagen fibrils [33–35] and can act as a mineralization promoter or inhibitor at low and high concentrations, respectively [36]. Our recent in vitro mineralization studies show that phosphorylated DPP induces organized mineralization of collagen fibrils in a concentration-dependent manner, while non-phosphorylated DPP stabilizes amorphous calcium phosphate (ACP) [37]. In addition to its role in biomineralization, DPP is involved in cell signaling and regulates cell differentiation [38,39]. The function of DSP in dentin matrix is less clear. No influence on mineralization has been observed in in vitro mineralization experiments [40] and no signaling function has been reported for this protein so far [11,41]. The role of DGP in dentin mineralization and whether it is present in species other than pig are unknown [41].

In the last decade, several studies of transgenic and knockout mice testing the function of DSP and DPP in dentinogenesis, but not amelogenesis, have been performed. Deletion of both copies of *Dspp* leads to a profound dentin phenotype, manifested by enlarged pulp cavities, wide predentin, and a hypomineralized dentin with mineralized calcospheres spread through the non-mineralized organic matrix [13,15,25,42,43]. Importantly, loss of only one copy of *Dspp* does not have significant effects on dentin [13,15,25,42,43]. This is intriguing since most DGI is inherited in an autosomal-dominant fashion. A potential explanation to this phenomenon is that the defects of DSPP in DGI cause disturbances of ER intracellular protein trafficking [24,44] and prevent secretion of ECM proteins, while only one normal allele of this gene is sufficient to maintain DSPP function in tooth matrix formation and mineralization. Our earlier studies showed that the mantle dentin is affected less than circumpulpal dentin [45], suggesting that DSPP is less involved in the formation of mantle dentin. One potential explanation for this phenomenon is that the process of mantle dentin mineralization process is different from the circumpulpal dentin. Namely, matrix vesicles are required for the mantle dentin mineralization [46], in contrast to the circumpulpal dentin which mineralizes at the mineralization front at the predentin–dentin boundary [2,33,47]. Interestingly enough, in human hypophosphatemic and hypocalcemic teeth, mantle is also affected less than circumpulpal dentin [48].

The importance of the proteolytic cleavage of DSPP into DPP and DSP has been demonstrated in an elegant experiment. The transgenic expression of the uncleavable D452A *Dspp* in the *Dspp*-null background did not rescue the null phenotype, indicating that the

proteolytic processing by extracellular proteinases is essential for the proper DSPP function [26]. To assess the role of DSP in dentinogenesis, Suzuki et al. [42] generated mice expressing DSP and a small portion of the C-terminal DGP under the control of the *Dspp* promoter in the *Dspp* KO background and observed a partial phenotype rescue. However, in a later study by Gibson et al. [49], the 3.6 Collagen I promoter driving the expression of a longer DSP fragment (N-terminus to the D452 cleavage site) resulted in a more severe phenotype than the *Dspp* KO. The length of DSP used or the tissue specificity of the promoters may explain the difference in phenotype [49,50].

Although DSPP is transiently expressed by polarized presecretory ameloblasts [17] its role in amelogenesis remains elusive. One of the reasons for this is that, to date, all of the studies of DSPP function have been conducted on mature animals, long after tooth mineralization. We have focused our current study on the developing mouse incisor (and un-erupted 1st molar) to precisely define the role of DSPP in biomineralization of dentin and enamel.

Materials and methods

Animals

***Dspp* mutant mice—**We collected mandibles from postnatal day 10 (P10), and one-month-old mice from the homozygote ($Dspp^{-/-}$) and heterozygote ($Dspp^{+/-}$) littermates [13]. For the in situ hybridization and immunohistochemistry experiments, timed pregnant CD-1 females were purchased from Charles River Laboratories. The plug date designated was embryonic day 0.5 (E0.5) and embryonic age (E15.5 to E18.5) was verified using morphological criteria. One-month-old C57BL/6 mice and one-month-old Wistar rats were purchased from Charles River Laboratories. In this study all animals were euthanized using carbon dioxide. All animal work was performed under and approved by the Institutional Animal Care and Usage Committees from the University of Pittsburgh, Hospital for Special Surgery and Baylor College of Medicine.

MicroCT studies

MicroCT data collection—The intact hemimandibles from one-month-old $Dspp^{+/-}$ (n = 6) and $Dspp^{-/-}$ (n = 6), were removed after euthanasia and fixed in 5% formalin overnight, followed by storage in 70% ethanol until analysis. Whole mandibles from 10 day-old $Dspp^{+/+}$ (n = 10) and $Dspp^{-/-}$ (n = 5) were stored in 70% ethanol until use. To enhance the microCT contrast and reduce artifacts from the surrounding bone, the molars were extracted from the mandible prior to the analysis.

All specimens were scanned on a Skyscan 1172 (Bruker-Skyscan, Contich, Belgium) microCT system in 70% ethanol. The hemimandibles from one-month-old mice and un-erupted molars from 10 day-old mice were mounted in a vertical position using Parafilm inside customized holders. Each scan included a set of mineral phantoms (0.25 and 0.75 g/cm^3) for mineral density calibration. The scans were conducted with a six-micron voxel size and 180 degree-angular range for all samples. The hemimandibles were scanned with a 60 KVp beam energy using a 0.5 mm Al filter, 800 ms exposure time and 10 frames per view. The first molars were scanned unfiltered with a 40 KVp beam energy, 300 ms

exposure time and 12 frames per view. The ReCon (Bruker-Skyscan) software system was used for reconstruction of the 3D volumes, provided as stacks of bmp images for every scan.

MicroCT-image processing—We reoriented the scan volumes of all the scans along the sagittal plane in a 3-plane-view mode using the DataViewer (Bruker-Skyscan) software. The images were digitally truncated to limit the volume to the areas surrounding incisors and saved as a separate file. The reoriented images were converted into dicom files and imported into the Scanco 3D morphometry and analysis software system (Scanco Medical, Bassersdorf, Switzerland), which operates in an open VMS environment. To assess enamel deposition and maturation rates, regions of interest (ROIs) were drawn around the enamel from the incisal edge through the cervical loop of the incisor, and around the entire enamel volume in the molar. The enamel regions of these images were binarized using the lowest threshold values and imported into the reoriented/truncated volumes generated on CTAn (version 1.13.5.1; Skyscan-Bruker). The CTAn microCT analysis software allows binary images to be imported as ROIs, and calculates the scan volumes using the bone mineral density phantoms (Bruker-Skyscan) for normalization. For the stepwise analysis of mineral deposition, we divided the entire incisor ROIs into 1 mm thick segments, and further sub-divided the 2 mm region adjacent to the cervical loop into 0.2 mm-long segments. The volume and average mineral density of enamel from both incisors and un-erupted molars were evaluated in CTAn using the lowest threshold values and reported as a function of segment distance from the onset of mineral deposition for the incisors and as an average from the whole crown for the molars.

Scanning Electron Microscopy

For backscattered SEM (BS SEM), after collection, the one-month-old hemimandibles were flash frozen in liquid nitrogen and freeze-dried. The dry samples were embedded in Epofix (EMS, Hatfield, PA). After polymerization, the incisors were sectioned into erupted and unerupted portions and polished using Isomet polisher (Buehler, Lake Bluff, IL) with a series of MetaDi™ Supreme polycrystalline diamond suspensions (Buehler, Lake Bluff, IL) down to 0.25 μm. The samples were carbon coated and studied using JSM 6335F SEM (Jeol, Peabody, MA).

For the measurements of enamel thickness, erupted portions of incisors from 7 animals from each group were embedded in Epofix and polished in the transverse plane as described above and etched with 10% EDTA for 5 s for easier identification of the outer and inner enamel layers. The samples were Au/Pl sputter coated and studied in secondary electron mode (SE SEM) using JSM6335F SEM (Jeol, Peabody, MA).

For resin casting, the mandibles were dissected and immersed in cold 70% ethanol overnight. The samples were further dehydrated in a stepwise series of ethanol and transferred into pure LRWhite resin (EMS, Hatfield, PA) and kept overnight. The resin was changed two more times with 24-h intervals. Resin polymerization was carried out at 60 °C for 48 h. The blocks were trimmed with glass and histological diamond knives to expose tooth surfaces, and etched with 37% phosphoric acid for 5 s and 5% sodium hypochlorite for

5 min. The sample blocks were then rinsed, air-dried, Au/Pl sputter coated and studied in SE SEM mode using JSM6335F SEM (Jeol, Peabody, MA).

Microhardness testing of enamel

Erupted portions of incisors from one-month-old *Dspp*$^{+/-}$ and *Dspp*$^{-/-}$ (n = 7/genotype) groups were air-dried and mounted in Epofix. The incisors were polished in the transverse plane as described above. The micro-indentation tests were conducted using IdentaMet 1105 microhardness tester with a CCD camera and OmniMet software (Buehler, Lake Bluff, Il). The tests were conducted using a Vickers diamond tip at 25 gf (0.24.5 N) load and 5 s dwell time. Five measurements were taken per sample at a distance of at least two indentation diagonals from each other and at roughly 20 μm from the DEJ along whole width of the enamel.

In situ hybridization

Briefly, the WT CD-1 mouse embryos were fixed overnight in 4% paraformaldehyde, dehydrated and infiltrated with paraffin. We cut 10 μm sections and placed on TESPA (triethoxysilylpropylamine) coated slides. The tissue was hybridized with an antisense probe to *Dspp* (a generous gift from Jifan Feng and Yang Chai, USC). The in situ hybridization was performed as described [51] and after the appropriate length of time for development, the sections were counterstained with eosin, mounted with Allen Scientific mounting media and covered by coverslips.

Immunohistochemistry

For Collagen IV immunohistochemistry, sections adjacent to those used for in situ hybridization were rehydrated and antigen retrieval was performed using citrate buffer. We incubated the sections overnight with the Collagen IV antibody (Abcam, 1:100). Signal was detected using the Vectastain kit. The slides were counterstained with methyl green, mounted with Allen Scientific mounting media and covered by coverslips.

Immunochemical visualization of DSP

For immunofluorescence microscopy of erupted portions of the incisors we used a published procedure [52]. Briefly, the erupted portions of the incisors from one-month-old wildtype mice were polished and incubated with 3% gelatin to seal dentinal tubules and other pores and repolished again to remove gelatin from the surface. The samples were etched in 2% EDTA and 1% paraformaldehyde solution for 5 min followed by a standard immunofluorescence staining procedure performed on the samples with 1/100 DSP antibodies (a generous gift from Dr. Larry Fisher, NIDCR, Bethesda, MD) with secondary anti-rabbit antibodies conjugated with Alexa-Fluor 594.

In addition to the immunofluorescence of mouse incisors we have conducted immunohistochemistry on rat incisors. The mandibles were dissected out of one-month-old Wistar rats after euthanasia and fixed in 4% paraformaldehyde. The samples were embedded in LR White and sectioned. The sections were demineralized using 5% EDTA and 2% paraformaldehyde solution and subjected to standard IHC procedure using DSP antibodies (a generous gift from Dr. Larry Fisher, NIDCR, Bethesda, MD).

Light microscopy

All in situ hybridization and collagen IV immunohistochemistry images were collected on a Zeiss Axioskop A1 and an MrC3 camera. The images of mouse and rat DSP were obtained using Nikon Eclipse light microscope in the bright field mode.2.9—.

Statistical analysis

The microCT and SEM data were analyzed using Students t-test and Analysis of Covariance ANCOVA in Excel and Origin Pro 9.1 software.

Results

Dspp$^{-/-}$ teeth demonstrate accelerated amelogenesis

To assess the contribution of DSPP to enamel formation we studied constantly growing incisors of one-month-old *Dspp* KO and heterozygous littermates in order to capture successive stages of amelogenesis in one specimen. No differences were observed in the incisor length between *Dspp*$^{+/-}$ and *Dspp*$^{-/-}$ in high-resolution microCT scans of one-month-old hemimandibles (Fig. 1A,C). In agreement with earlier studies [13,45,49], the dentin layer of the *Dspp* knockout was much thinner and shows the characteristic spherulitic mineralized bodies with large hypomineralized interglobular areas between them (Fig. 1B). Intriguingly, we observed that the onset of enamel deposition occurs much closer to the cervical loop in the *Dspp*$^{-/-}$ incisors compared to the heterozygotes, 560 vs. 790 μm ($p = 0.03$) from the cervical loop respectively (Fig. 1C,D; Suppl. Fig. 1).

We were able to quantify the enamel mineral density for all stages of amelogenesis and enamel biomineralization in the incisor. No detectable difference in density between *Dspp* genotypes was observed in the mature enamel (4–8 mm from the onset of enamel deposition, Fig. 2A). The *Dspp*$^{-/-}$ maturation stage enamel, 3 and 4 mm from onset of enamel deposition, is significantly denser than that of the heterozygote control mouse (Table 1, Fig. 2A). We noticed a marginal difference in the density values in the segment containing the 2nd mm from the onset of enamel deposition (Fig. 2A). We further carried out a study of the first 2 mm from the onset of enamel deposition with smaller intervals of 0.2 mm, which revealed that the mineral density of the *Dspp*$^{-/-}$ enamel was significantly higher than in *Dspp*$^{+/-}$ at a distance from 1.4 to 2.0 mm from the onset of enamel deposition, which corresponds to the late secretory stage (Table 1, Fig. 2B).

We also analyzed the enamel volume along the forming incisor to determine the rate of enamel deposition (Fig. 3A,B). In the early/mid-secretory stage enamel, the *Dspp*$^{-/-}$ enamel volume is significantly higher than in the *Dspp*$^{+/-}$ (Table 1, Fig. 3B). However, this situation is reversed at the late secretory stage where the volume of *Dspp*$^{+/-}$ enamel is higher than that of *Dspp*$^{-/-}$ and it stays significantly higher until eruption (Table 1, Fig. 3A,B). It is important to notice that the smaller enamel volumes cannot be interpreted simply as a decrease in the enamel deposition, as the cross-sections of incisors of the KO mice are smaller and have a lower labial surface width, which accounts for much of the volume difference.

We assessed the rate of enamel deposition by measuring the enamel thickness along the developing incisor (Fig. 3C). Similar to the volume data, the *Dspp*$^{-/-}$ incisors have thicker enamel during the early and mid-secretory stage of amelogenesis, (0.0–1.2 mm; ANCOVA, $p = 0.03$). In the distal region, the thicknesses of the *Dspp*$^{+/-}$ and *Dspp*$^{-/-}$ enamel become similar. These observations indicate that the *Dspp*$^{-/-}$ mice secrete more enamel matrix over a shorter time period compared to the *Dspp*$^{+/-}$.

To further test the hypothesis that maturation of enamel is affected by loss of DSPP in all tooth types and not only in the incisors we studied the unerupted 1st molars of 10 day-old mice. Since these are un-erupted teeth potential differences due to the difference in the rate of enamel attrition can be ruled out. We observed a larger volume of higher mineral density enamel in the *Dspp*$^{-/-}$ compared to their *Dspp*$^{+/-}$ counterparts (Fig. 4). This suggests that enamel maturation in the mutant molars is expedited. We performed statistical analysis of the volume values in the density region from 1.5–2.0 g/cm^3 and found that these differences were significantly different ($p < 0.05$). These results are in agreement with the incisor results that support a role for DSPP in the enamel formation.

Microstructure of the enamel at the enamel-dentin interface affected by loss of DSPP

We have assessed the differences in the microstructure of enamel and DEJ between the *Dspp*$^{-/-}$ and *Dspp*$^{+/-}$ using SEM. SEM studies reveal that the surface enamel layer is significantly thinner in *Dspp*$^{-/-}$ compared with that of *Dspp*$^{+/-}$ (Fig. 5). Similarly, the ratio of the surface enamel thickness to full enamel thickness is significantly smaller in *Dspp*$^{-/-}$. One potential reason for the decreased thickness of the outer enamel is the shortening of the secretory stage resulting in the early cessation of the surface enamel deposition. These observations are in agreement with the results of the microCT analysis showing shortened secretory stage in DSPP KO incisors. There was also a difference in the organization of the inner enamel layer. Specifically, the prisms in the inner 10 μm of enamel were roughly parallel to each other and oriented normal to the DEJ and did not form a quasi-orthogonal pattern typical of murine incisal enamel (Fig. 5A,B).

Backscattered SEM (BS SEM) studies of the erupted portions of the incisors revealed a major phenotype at the dentin-enamel junction (DEJ) (Fig. 6). The interface between dentin and enamel is compromised in the *Dspp*$^{-/-}$, leading to delamination of these tissues (Fig. 6A). In contrast, in *Dspp*$^{+/-}$ this interface remains intact, even next to a major crack (an artifact of drying) running through the DEJ from dentin into enamel (Suppl. Fig. 2). Linear defects of mineralization in a form of 500 nm wide lines of under-mineralized dentin running along the DEJ plane were prominent in the *Dspp*$^{-/-}$. This type of mineralization defect is different from characteristic globular mineralization of circumpulpal dentin in *Dspp* mutants [13,26,42,45,49].

We noticed in the BS SEM of polished incisors that the diameters of the dentinal tubules in the mantle dentin adjacent to enamel are larger and there is much less tubule branching in the *Dspp* mutants. To further study the morphology of odontoblast processes at the DEJ we performed SEM of resin cast samples in the secondary electron (SE) mode. The studies of resin casted and etched samples by SE SEM revealed a dense network of extensively branching thin odontoblast processes in the *Dspp*$^{+/-}$ (Fig. 6A,C). In contrast the odontoblast

processes in *Dspp*$^{-/-}$ were significantly thicker, 1.4 μm (±0.25) vs. 0.58 μm (±0.14) ($p = 3.37 \times 10^{-7}$) and the branching was almost nonexistent (Fig. 6B,D).

To further test the hypothesis that DSPP plays a role at the DEJ we conducted immunohistochemical studies using DSP antibodies on fully mineralized erupted incisors from one-month-old wild type mice and demineralized resin sections of rat incisors. Both techniques detected a strong DSP signal at the DEJ in *Dspp*$^{+/+}$ (Fig. 7, Suppl. Fig. 3).

Microhardness of mature enamel is unaffected by the lack of *Dspp*

Microhardness tests revealed no significant differences between heterozygotes and DSPP KO samples, HV = 286 ± 15.61 vs. 291 ± 15.31 ($p = 0.73$) respectively, indicating that the absence of DSPP does not affect the structure and the degree of mineralization of enamel. These results are in agreement with the microCT and SEM observations showing no difference in the mineral density and structural organization of the distal region mature enamel between heterozygous and DSPP KO mice.

Dspp mRNA is expressed by secretory ameloblasts

The results of our microCT and SEM studies point to a potential role of DSPP in secretory enamel. Yet, previous reports indicate that DSPP is only transiently expressed in presecretory ameloblasts [17,18]. We decided to take a second look at the expression of (mRNA) *Dspp* in ameloblasts, and assayed its expression from embryonic day E15.5 to birth. The earliest expression by in situ hybridization was observed in the E16.5 incisor (Fig. 8A, Table 2) where *Dspp* mRNA is expressed in both ameloblast and odontoblast cell layers. To identify preameloblast–ameloblast transition we performed immunohistochemistry for Collagen IV on adjacent sections. Collagen IV is the major component of basement lamina, which is lysed by ameloblasts prior to secretion of enamel [2]. Collagen IV staining was associated with earlier phases of the (mRNA) *Dspp* expression in ameloblasts, in agreement with earlier observations (Fig. 8B). At the same time, we observed its expression throughout the ameloblast layer in which basal lamina is absent. Therefore, we conclude that (mRNA) *Dspp* is expressed not only in presecretory ameloblasts but also during enamel formation. At E18.5, the expression of (mRNA) *Dspp* was observed throughout the odontoblast layer, however only the most apical ameloblasts expressed *Dspp* mRNA. These data indicate that (mRNA) *Dspp* expression is confined to presecretory and early secretory ameloblasts. In our experiments, (mRNA) *Dspp* expression did not initiate until 2 days later, at E18.5, in the mandibular first molars (Suppl. Fig. 4).

Discussion

The focus of our study was to obtain new insights on the role of DSPP in tooth development with a specific focus on the enamel formation. We made several novel observations and for the first time demonstrated the effects of DSPP on amelogenesis. Specifically, we found that in the absence of DSPP enamel deposition begins earlier and both enamel secretion and maturation are accelerated. Furthermore, we found that the outer enamel layer in *Dspp*$^{-/-}$ incisors is thinner and the DEJ is compromised. We also observed that odontoblast processes in mantle dentin adjacent to enamel are thicker and branch less in *Dspp*$^{-/-}$ than in the

Dspp$^{+/-}$. Importantly, (mRNA) *Dspp* expression in secretory ameloblasts of the incisors was detected for the first time, suggesting that the observed phenotype is caused by the endogenous expression of (mRNA) *Dspp* during the secretory stage of amelogenesis.

Using incisors as a model our study revealed a number of novel aspects of DSPP function. Specifically, our microCT analysis demonstrates that in the absence of DSPP amelogenesis starts earlier, based on the fact that the first mineralized enamel layer appears significantly closer to the cervical loop. This finding suggests that DSPP functions as a coordinator of the onset of enamel formation during odontogenesis, during which the sequence of dentin and enamel deposition is tightly coordinated [2]. Dentin is normally deposited and starts to mineralize first. Once a certain thickness of dentin (typically mantle dentin) is deposited, the breakdown of basal lamina takes place followed by the initiation of enamel deposition on the surface of the mineralized dentin. Since this sequence is present in all mammalian species studied it is critical for a proper tooth formation and function. In *Dspp* KO the coordination of dentin and enamel development is compromised and the onset of enamel formation is premature, which likely causes a weak dentin-enamel interface observed in this animal model.

The microCT analysis revealed a higher rate of enamel deposition and expedited maturation of enamel in the *Dspp*$^{-/-}$ incisors when compared to the heterozygous counterparts. The differences are transient and eventually both mineral density and enamel thickness values in *Dspp*$^{+/-}$ and *Dspp*$^{-/-}$ incisors become equal. Our observations are also supported by the microhardness tests and the SEM analysis, which show no difference in hardness and thickness of mature enamel between *Dspp* heterozygotes and homozygotes. At the same time using SEM we identified a number of differences in the enamel structural organization. Specifically, we demonstrate that although the overall thickness of mature enamel in *Dspp*$^{-/-}$ is not different that in the *Dspp*$^{+/-}$, the surface layer of enamel is thinner in the DSPP KO incisors, while the middle and inner enamel layers make up the remainder of the volume. These results indicate that in the absence of DSPP, the differentiation of ameloblasts is accelerated and the enamel secretion occurs at a higher rate during early and mid-secretory stage when (mRNA) *Dspp* is expressed. The fact that in the *Dspp*$^{-/-}$ enamel rods are organized normal to the DEJ in the inner enamel layer, might suggest that the secretory ameloblasts are not fully differentiated at this point and their Tomes' processes are not fully formed. At the same time the reduction in the surface enamel thickness indicates that secretion of enamel ceases and maturation begins earlier, before the full thickness of the surface enamel is deposited. This suggests that differentiation from secretory to maturation ameloblasts DSPP might be involved in the secretory-maturation transition, which is an intriguing hypothesis, since no *Dspp* mRNA is observed in ameloblasts during this transition.

Our study for the first time demonstrates (mRNA) *Dspp* expression in the secretory ameloblasts of mouse incisors. We observed the expression of (mRNA) *Dspp* in the secretory ameloblasts from incisors at E16.5 to E18.5, and P10 while previous studies have only detected its expression in presecretory ameloblasts, prior to the onset of dentin deposition in both molars and incisors [17,18,20]. This observation is important since it provides a biological basis for our observations of changes in the enamel secretion and

maturation. Expression of *Dspp* in ameloblasts is usually described as transient [17,20]. Indeed, in the majority of tooth types its expression by ameloblasts is transient and ceases as these teeth mature. However, since incisors are constantly forming and contain all stages of differentiation at any given time they express (mRNA) *Dspp* and all other genes involved in odontogenesis throughout the life of the animal, while individual ameloblasts express (mRNA) *Dspp* transiently, as they progress through the successive stages of amelogenesis.

Put together, our results strongly suggest that DSPP may be involved in ameloblast differentiation and physiology via cell signaling. The tissue culture experiments demonstrate that DPP activates numerous signaling pathways [38,39,53]. Similarly, DSP has been shown to induce differentiation of pulp stem cells [54]. Hence, it is possible that DSPP is involved in the regulation of ameloblast differentiation and physiological activity, however additional studies are needed to test this hypothesis.

The dentin phenotype in $Dspp^{-/-}$ animals has been thoroughly characterized over the years and it has been shown that both major cleavage products of DSPP play a major role in dentinogenesis [13,26,42,49,55]. It has been also found in the alveolar bone [14] and the loss of DSPP is associated with periodontal disease [43]. In this study, for the first time, we demonstrate that DSPP plays a role in amelogenesis. We were able to identify the enamel phenotype through high-resolution microCT analysis of all stages of amelogenesis in the young incisor. We chose this approach because previous studies focused on the phenotype of mature $Dspp^{-/-}$, teeth, and did not include earlier stages of tooth development [13,26,42,43,55,56]. Accordingly, although the mature portions of the incisors did not have major enamel structural or functional defects except a weak DEJ and thinner outer enamel, there were clear differences during the secretory and maturation stages. Recently, hypoplastic enamel phenotypes were described in two unrelated families with DGI-II caused by dominant-negative mutations in *DSPP* [27]. The authors hypothesized that this dominant-negative effect is due to the cellular pathologies of pre-ameloblasts. However, in light of our finding of (mRNA) *Dspp* expression at the secretory stage of enamel formation and changes in the rates of enamel deposition and maturation one should consider the effects of these mutations at the later stages of enamel formation.

Our current results show a weaker interface between dentin and enamel in the $DSPP^{-/-}$. Since DSPP is expressed in odontoblasts and pre-secretory and secretory ameloblasts during the formation of the DEJ, these data support the notion that DSPP plays an important role in the formation of this interface. We have previously shown that there is an extremely high degree of alignment between mineral crystals of dentin and enamel although direct epitaxy is very rare [57]. It has been proposed that mineral formation and alignment at the dentin-enamel boundary are regulated by integrated organic matrices of dentin and enamel [57]. It is plausible that DSPP functions in these integrated organic matrices at the DEJ. Our immunohistochemical observations of DSP at the DEJ further support this notion. Alternatively, the DEJ defect might be related to the earlier onset of enamel deposition in the $Dspp^{-/-}$. In $Dspp^{-/-}$ according to our results the coordination of dentin and enamel development is compromised and we hypothesize that this leads to a weak dentin-enamel interface.

Another major feature of the *Dspp*$^{-/-}$ dentin is the significant reduction in branching and the increase in width of the odontoblast processes. Altered phenotype including the reduced branching has been previously described in mandibular osteocytes of the *Dspp*$^{-/-}$ mice [43]. Reduction in the branching and changes in the odontoblast process morphology suggest that the odontoblastic transport to the DEJ is compromised. This lack of proper transport can potentially affect the delivery of mineral and matrix molecules towards the DEJ, impede signaling from odontoblasts to presecretory and early secretory ameloblast, and further contribute to the weakness of this interface in the *Dspp*$^{-/-}$ animals.

Conclusions

In conclusion, the results of our study demonstrate that lack of DSPP causes changes in amelogenesis. We show that the onset of amelogenesis in *Dspp*$^{-/-}$ is shifted earlier and both secretory and maturation stages of amelogenesis are accelerated. Importantly, these differences are transient and only minor phenotypic traits were observed in the mature enamel. We show that (mRNA) *Dspp* is expressed in early secretory ameloblasts, and this expression is likely responsible for regulation of ameloblasts differentiation and their cell physiology. Finally we observed major defects of the DEJ in *Dspp*$^{-/-}$ incisors, which might be caused by several factors including the lack of DSPP cleavage products at the site of DEJ, an earlier onset of enamel deposition or a compromised transport of mineral and proteins through malformed odontoblast processes. Our data provide a new perspective on the function of DSPP in odontogenesis and highlight an importance of the studies of biomineralization process throughout all stages of tissue formation.

Supplementary Material

Refer to Web version on PubMed Central for supplementary material.

Acknowledgments

The authors are grateful for the support by NIH — DE016703 (EB), DE020740 (HLSR, KV), DE04141 (ALB, KV) AR037661 (ALB) and DE022549 (CQ), and start-up funds from the University of Pittsburgh School of Dental Medicine (HLSR, KV). We thank Dr. Jifan Feng and Dr. Yang Chai from USC for the (mRNA) *Dspp* probe construct. The microCT data were collected at the Allegheny General Hospital microCT core facility (Pittsburgh, PA). The SEM studies described in this project were conducted at the Center for Biological Imaging, University of Pittsburgh (Pittsburgh, PA).

References

1. Jernvall J, Thesleff I. Reiterative signaling and patterning during mammalian tooth morphogenesis. Mech. Dev. 2000; 92:19–29. [PubMed: 10704885]
2. Ten, NA. Structure, and Function. Mosby; St. Luis: 2007. Cate's Oral Histology: Development.
3. Takano Y, Sakai H, Baba O, Terashima T. Differential involvement of matrix vesicles during the initial and appositional mineralization processes in bone, dentin, and cementum. Bone. 2000; 26:333–339. [PubMed: 10719275]
4. Zaslansky P, Friesem AA, Weiner S. Structure and mechanical properties of the soft zone separating bulk dentin and enamel in crowns of human teeth: insight into tooth function. J. Struct. Biol. 2006; 153:188–199. [PubMed: 16414277]
5. Simmer JP, Hu JCC. Expression, structure, and function of enamel proteinases. Connect. Tissue Res. 2002; 43:441–449. [PubMed: 12489196]

6. Fukae M, Yamamoto R, Karakida T, Shimoda S, Tanabe T. Micelle structure of amelogenin in porcine secretory enamel. J. Dent. Res. 2007; 86:758–763. [PubMed: 17652206]
7. MacDougall M, Simmons D, Luan XH, Nydegger J, Feng J, Gu TT. Dentin phosphoprotein and dentin sialoprotein are cleavage products expressed from a single transcript coded by a gene on human chromosome 4 — dentin phosphoprotein DNA sequence determination. J. Biol. Chem. 1997; 272:835–842. [PubMed: 8995371]
8. Fisher LW, Torchia DA, Fohr B, Young MF, Fedarko NS. Flexible structures of SIBLING proteins, bone sialoprotein, and osteopontin. Biochem. Biophys. Res. Commun. 2001; 280:460–465. [PubMed: 11162539]
9. Fisher LW, Fedarko NS. Six genes expressed in bones and teeth encode the current members of the SIBLING family of proteins. Connect. Tissue Res. 2003; 44:33–40. [PubMed: 12952171]
10. Zhang XH, Zhao J, Li CF, Gao S, Qiu CC, Liu P, et al. DSPP mutation in dentinogenesis imperfecta shields type II. Nat. Genet. 2001; 27:151–152. [PubMed: 11175779]
11. Qin C, Baba O, Butler WT. Post-translational modifications of sibling proteins and their roles in osteogenesis and dentino-genesis. Crit. Rev. Oral Biol. Med. 2004; 15:126–136. [PubMed: 15187031]
12. Kim JW, Simmer JP, Hereditary dentin defects J. Dent. Res. 2007; 86:392–399.
13. Sreenath T, Thyagarajan T, Hall B, Longenecker G, D'Souza R, Hong S, et al. Dentin sialophosphoprotein knockout mouse teeth display widened predentin zone and develop defective dentin mineralization similar to human dentinogenesis imperfecta type III. J. Biol. Chem. 2003; 278:24874–24880. [PubMed: 12721295]
14. Baba O, Qin CL, Brunn JC, Jones JE, Wygant JN, McIntyre BW, et al. Detection of dentin sialoprotein in rat periodontium. Eur. J. Oral Sci. 2004; 112:163–170. [PubMed: 15056114]
15. Liu Q, Gibson MP, Sun H, Qin C. Dentin sialophosphoprotein (DSPP) plays an essential role in the postnatal development and maintenance of mouse mandibular condylar cartilage. J. Histochem. Cytochem. 2013; 61:749–758. [PubMed: 23900597]
16. Sun Y, Ma S, Zhou J, Yamoah AK, Feng JQ, Hinton RJ, et al. Distribution of small integrin-binding ligand, N-linked glycoproteins (SIBLING) in the articular cartilage of the rat femoral head. J. Histochem. Cytochem. 2010; 58:1033–1043. [PubMed: 20679519]
17. Begue-Kirn C, Krebsbach PH, Bartlett JD, Butler WT. Dentin sialoprotein, dentin phosphoprotein, enamelysin and ameloblastin: tooth-specific molecules that are distinctively expressed during murine dental differentiation. Eur. J. Oral Sci. 1998; 106:963–970. [PubMed: 9786327]
18. Bleicher F, Couble ML, Farges JC, Couble P, Magloire H. Sequential expression of matrix protein genes in developing rat teeth. Matrix Biol. 1999; 18:133–143. [PubMed: 10372553]
19. MacDougall M, Gu TT, Luan XG, Simmons D, Chen JK. Identification of a novel isoform of mouse dentin matrix protein 1: spatial expression in mineralized tissues. J. Bone Miner. Res. 1998; 13:422–431. [PubMed: 9525343]
20. D'Souza RN, Cavender A, Sunavala G, Alvarez J, Ohshima T, Kulkarni AB, et al. Gene expression patterns of murine dentin matrix protein 1 (Dmp1) and dentin sialophosphoprotein (DSPP) suggest distinct developmental functions in vivo. J. Bone Miner. Res. 1997; 12:2040–2049. [PubMed: 9421236]
21. Butler WT. Dentin matrix proteins. Eur. J. Oral Sci. 1998; 106:204–210. [PubMed: 9541227]
22. Yamakoshi Y, Hu JCC, Iwata T, Kobayashi K, Fukae M, Simmer JP. Dentin sialophosphoprotein is processed by MMP-2 and MMP-20 in vitro and in vivo. J. Biol. Chem. 2006; 281:38235–38243. [PubMed: 17046814]
23. Hu JCC, Hu YY, Lu YH, Smith CE, Lertlam R, Wright JT, et al. Enamelin is critical for ameloblast integrity and enamel ultrastructure formation. PLoS One. 2014; 9
24. von Marschall Z, Fisher LW. Dentin sialophosphoprotein (DSPP) is cleaved into its two natural dentin matrix products by three isoforms of bone morphogenetic protein-1 (BMP1). Matrix Biol. 2010; 29:295–303. [PubMed: 20079836]
25. Sun Y, Lu Y, Chen S, Prasad M, Wang X, Zhu Q, et al. Key proteolytic cleavage site and full-length form of DSPP. J. Dent. Res. 2010; 89:498–503. [PubMed: 20332332]

26. Zhu Q, Gibson MP, Liu Q, Liu Y, Lu Y, Wang X, et al. Proteolytic processing of dentin sialophosphoprotein (DSPP) is essential to dentinogenesis. J. Biol. Chem. 2012; 287:30426–30435. [PubMed: 22798071]
27. Wang SK, Chan HC, Rajderkar S, Milkovich RN, Uston KA, Kim JW, et al. Enamel malformations associated with a defined dentin sialophosphoprotein mutation in two families. Eur. J. Oral Sci. 2011; 119:158–167. [PubMed: 22243242]
28. Yamakoshi Y, Nagano T, Hu JCC, Yamakoshi F, Simmer JP. Porcine dentin sialoprotein glycosylation and glycosaminoglycan attachments. BMC Biochem. 2011; 12
29. Yamakoshi Y, Hu JCC, Fukae M, Iwata T, Kim J-W, Zhang H, et al. Porcine dentin sialoprotein is a proteoglycan with glycosaminoglycan chains containing chondroitin 6-sulfate. J. Biol. Chem. 2005; 280:1552–1560. [PubMed: 15537641]
30. Qin C, Jan CB, Otto B, James NW, Bradley WM, William TB. Dentin sialoprotein isoforms: detection and characterization of a high molecular weight dentin sialoprotein. Eur. J. Oral Sci. 2003; 111:235–242. [PubMed: 12786955]
31. Zhu Q, Sun Y, Prasad M, Wang X, Yamoah AK, Li Y, et al. Glycosaminoglycan chain of dentin sialoprotein proteoglycan. J. Dent. Res. 2010; 89:808–812. [PubMed: 20400719]
32. Stetler-Stevenson W, Veis A. Bovine dentin phosphophoryn: calcium ion binding properties of a high molecular weight preparation. Calcif. Tissue Int. 1987; 40:97–102. [PubMed: 3105840]
33. Beniash E, Traub W, Veis A, Weiner S. A transmission electron microscope study using vitrified ice sections of predentin: structural changes in the dentin collagenous matrix prior to mineralization. J. Struct. Biol. 2000; 132:212–225. [PubMed: 11243890]
34. Dahl T, Sabsay B, Veis A. Type I collagen-phosphophoryn interactions: specificity of the monomer-monomer binding. J. Struct. Biol. 1998; 123:162–168. [PubMed: 9843670]
35. Stetler-Stevenson W, Veis A. Type I collagen shows a specific binding affinity for bovine dentin phosphophoryn. Calcif. Tissue Int. 1986; 38:135–141. [PubMed: 3011229]
36. Boskey AL, Maresca M, Doty SB, Sabsay B, Veis A. Concentration-dependent effects of dentin phosphophoryn in the regulation of in vitro hydroxyapatite formation and growth. Bone Miner. 1990; 11:55–65. [PubMed: 2176557]
37. Deshpande AS, Fang P-A, Zhang X, Jayaraman T, Sfeir C, Beniash E. Primary structure and phosphorylation of dentin matrix protein 1 (DMP1) and dentin phosphophoryn (DPP) uniquely determine their role in biomineralization. Biomacromolecules. 2011; 12:2933–2945. [PubMed: 21736373]
38. Jadlowiec J, Koch H, Zhang XY, Campbell PG, Seyedain M, Sfeir C. Phosphophoryn regulates the gene expression and differentiation of NIH3T3, MC3T3-E1, and human mesenchymal stem cells via the integrin/MAPK signaling pathway. J. Biol. Chem. 2004; 279:53323–53330. [PubMed: 15371433]
39. Eapen A, Ramachandran A, George A. Dentin phospho-protein (DPP) activates integrin-mediated anchorage-dependent signals in undifferentiated mesenchymal cells. J. Biol. Chem. 2012; 287:5211–5224. [PubMed: 22134916]
40. Boskey A, Spevak L, Tan M, Doty SB, Butler WT. Dentin sialoprotein (DSP) has limited effects on in vitro apatite formation and growth. Calcif. Tissue Int. 2000; 67:472–478. [PubMed: 11289697]
41. Prasad M, Butler WT, Qin CL. Dentin sialophosphoprotein in biomineralization. Connect. Tissue Res. 2010; 51:404–417. [PubMed: 20367116]
42. Suzuki S, Sreenath T, Haruyama N, Honeycutt C, Terse A, Cho A, et al. Dentin sialoprotein and dentin phosphoprotein have distinct roles in dentin mineralization. Matrix Biol. 2009; 28:221–229. [PubMed: 19348940]
43. Gibson MP, Zhu Q, Liu Q, D'Souza RN, Feng JQ, Qin C. Loss of dentin sialophosphoprotein leads to periodontal diseases in mice. J. Periodontal Res. 2012 n/a.
44. von Marschall Z, Mok S, Phillips MD, McKnight DA, Fisher LW. Rough endoplasmic reticulum trafficking errors by different classes of mutant dentin sialophosphoprotein (DSPP) cause dominant negative effects in both dentinogenesis imperfecta and dentin dysplasia by entrapping normal DSPP. J. Bone Miner. Res. 2012; 27:1309–1321. [PubMed: 22392858]

45. Fang PA, Verdelis K, Yang X, Lukashova L, Boskey AL, Beniash E. Ultrastructural organization of dentin in mice lacking dentin sialo-phosphoprotein. Connect. Tissue Res. 2014; 55:92–96. [PubMed: 25158189]
46. Golub EE. Role of matrix vesicles in biomineralization. Biochim. Biophys. Acta Gen. Subj. 2009; (1790):1592–1598.
47. Goldberg M, Rapoport O, Septier D, Palmier K, Hall R, Embery G, et al. Proteoglycans in predentin: the last 15 micrometers before mineralization. Connect. Tissue Res. 2003; 44:184–188. [PubMed: 12952195]
48. Foster BL, Nociti FH, Somerman MJ. The rachitic tooth. Endocr. Rev. 2014; 35:1–34. [PubMed: 23939820]
49. Gibson MP, Liu QL, Zhu QL, Lu YB, Jani P, Wang XF, et al. Role of the NH2-terminal fragment of dentin sialophosphoprotein in dentinogenesis. Eur. J. Oral Sci. 2013; 121:76–85. [PubMed: 23489896]
50. Paine ML, Luo W, Wang HJ, Bringas P, Ngan AYW, Miklus VG, et al. Dentin sialoprotein and dentin phospho-protein overexpression during amelogenesis. J. Biol. Chem. 2005; 280:31991–31998. [PubMed: 16014627]
51. Tabler Jacqueline M, Barrell William B, Szabo-Rogers Heather L, Healy C, Yeung Y, Perdiguero Elisa G, et al. Fuz mutant mice reveal shared mechanisms between ciliopathies and FGF-related syndromes. Dev. Cell. 2013; 25:623–635. [PubMed: 23806618]
52. Beniash E, Deshpande AS, Fang PA, Lieb NS, Zhang X, Sfeir CS. Possible role of DMP1 in dentin mineralization. J. Struct. Biol. 2011; 174:100–106. [PubMed: 21081166]
53. Jadlowiec JA, Zhang XY, Li JH, Campbell PG, Sfeir C. Extracellular matrix-mediated signaling by dentin phosphophoryn involves activation of the smad pathway independent of bone morphogenetic protein. J. Biol. Chem. 2006; 281:5341–5347. [PubMed: 16326713]
54. Lee SY, Kim SY, Park SH, Kim JJ, Jang JH, Kim EC. Effects of recombinant dentin sialoprotein in dental pulp cells. J. Dent. Res. 2012; 91:407–412. [PubMed: 22269273]
55. Gibson MP, Zhu Q, Wang S, Liu Q, Liu Y, Wang X, et al. The rescue of dentin matrix protein 1 (DMP1)-deficient tooth defects by the transgenic expression of dentin sialophosphoprotein (DSPP) indicates that DSPP is a downstream effector molecule of DMP1 in dentinogenesis. J. Biol. Chem. 2013; 288:7204–7214. [PubMed: 23349460]
56. Verdelis K, Ling Y, Sreenath T, Haruyama N, MacDougall M, van der Meulen MCH, et al. DSPP effects on in vivo bone mineralization. Bone. 2008; 43:983–990. [PubMed: 18789408]
57. Fang PA, Lam RSK, Beniash E. Relationships between dentin and enamel mineral at the dentino-enamel boundary: electron tomography and high-resolution transmission electron microscopy study. Eur. J. Oral Sci. 2011; 119:120–124. [PubMed: 22243237]

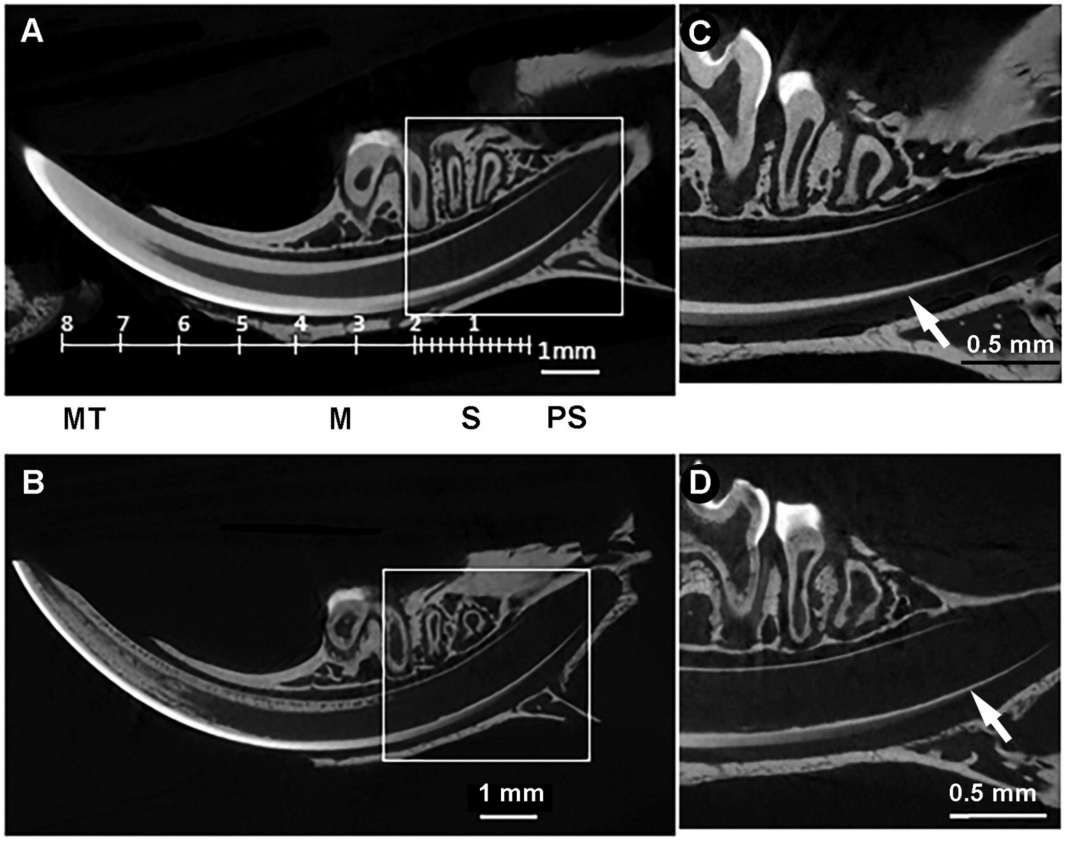

Fig. 1.

Enamel mineralization occurs precociously in the *Dspp*$^{-/-}$ incisor. MicroCT reconstructions of mandibles from one-month-old *Dspp*$^{+/-}$ (**A, C**) and *Dspp*$^{-/-}$ (**B, D**) mice. **A** and **B** represent sagittal views of whole jaw, note that incisor volumes were oriented to fit the whole incisor length. And **C** and **D** are close ups from the cervical parts of the incisors in the boxed areas of **A** and **B**; arrows pointing to the onset of amelogenesis. M — Maturation; MT — Mature; PS — Presecretory; S — Secretory.

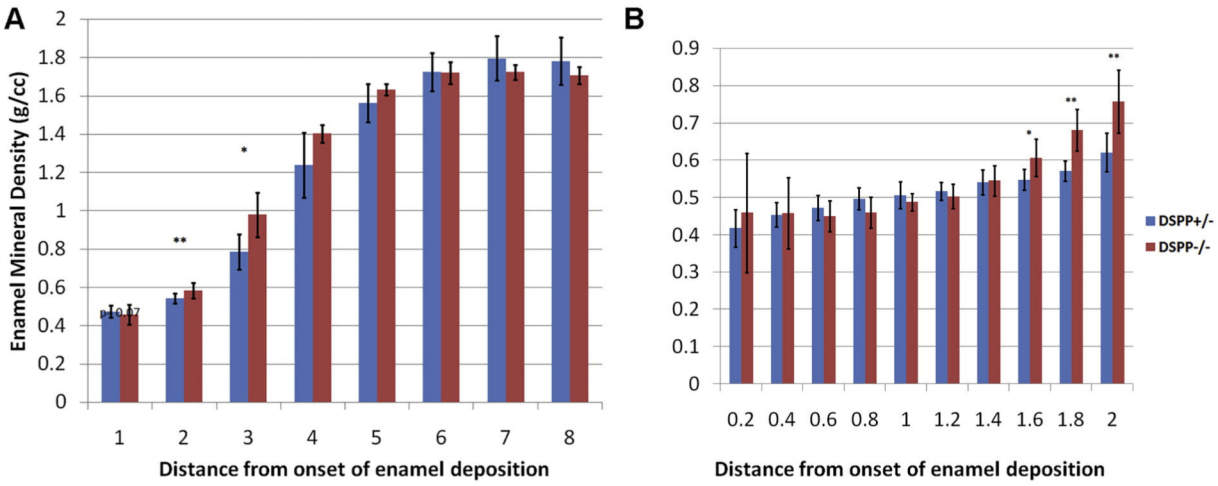

Fig. 2.

Dspp$^{-/-}$ enamel has increased mineral density in the early secretory phase. Enamel mineral density profiles from one-month-old DSPP *Dspp*$^{+/-}$ (**red**) and *Dspp*$^{-/-}$ (**blue**) mouse **A**) whole incisor profile using 1 mm thick segments along the incisor axis and **B**) high resolution profile of first 2 mm of forming enamel using 0.2 mm thick segments along the incisor axis. The statistically significant differences are marked with asterisks: *–$p < 0.05$, **–$p < 0.01$. (For interpretation of the references to color in this figure legend, the reader is referred to the web version of this article.)

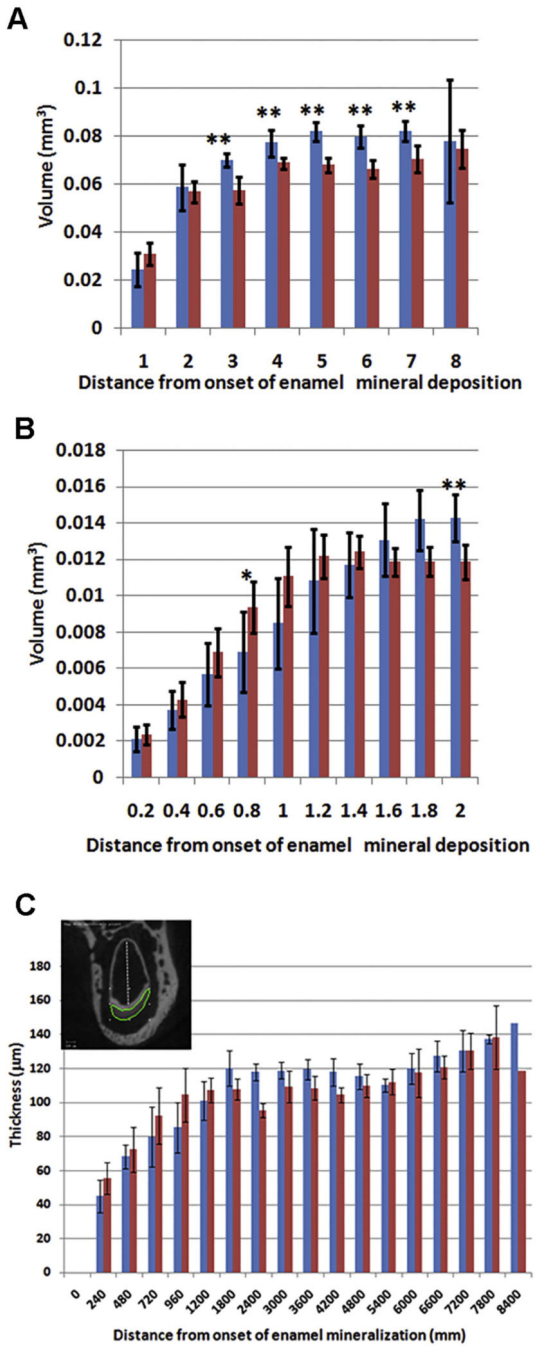

Fig. 3.

Dspp$^{-/-}$ enamel its maximum volume prematurely. **A** and **B** enamel volume profiles from one-month-old DSPP *Dspp*$^{+/-}$ (**red**) and *Dspp*$^{-/-}$ (**blue**) mouse — (**A**) whole incisor profile using 1 mm thick segments along the incisor axis and (**B**) high resolution profile of first 2 mm of forming enamel using 0.2 mm thick segments along the incisor axis. **C**. Enamel thickness profile. The inset marks the line along which the measurements were carried out. The statistically significant differences are marked with asterisks: *–$p < 0.05$, **–$p < 0.01$.

(For interpretation of the references to color in this figure legend, the reader is referred to the web version of this article.)

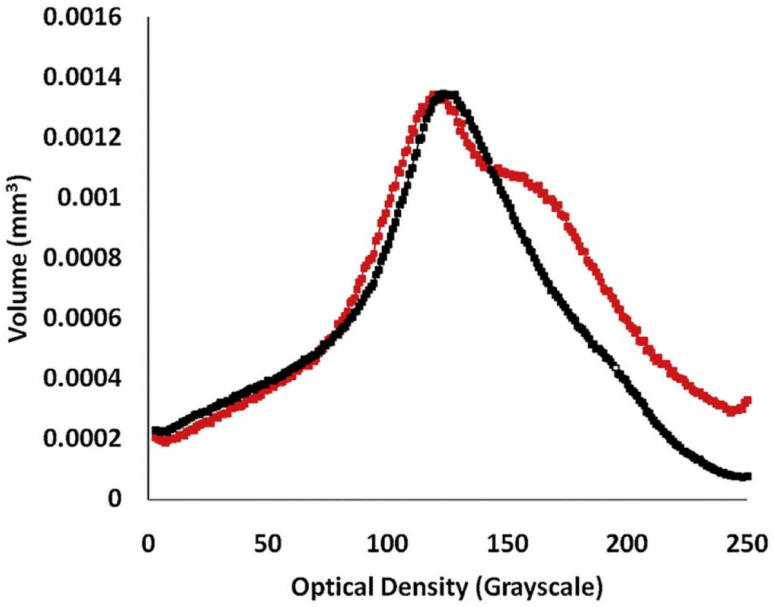

Fig. 4.

Unerupted *Dspp*$^{-/-}$ molars have increased mineral density. Distribution of enamel mineral density in 1st molars from 10 day-old *Dspp*$^{+/+}$ (black) and *Dspp*$^{-/-}$ (red) mice. (For interpretation of the references to color in this figure legend, the reader is referred to the web version of this article.)

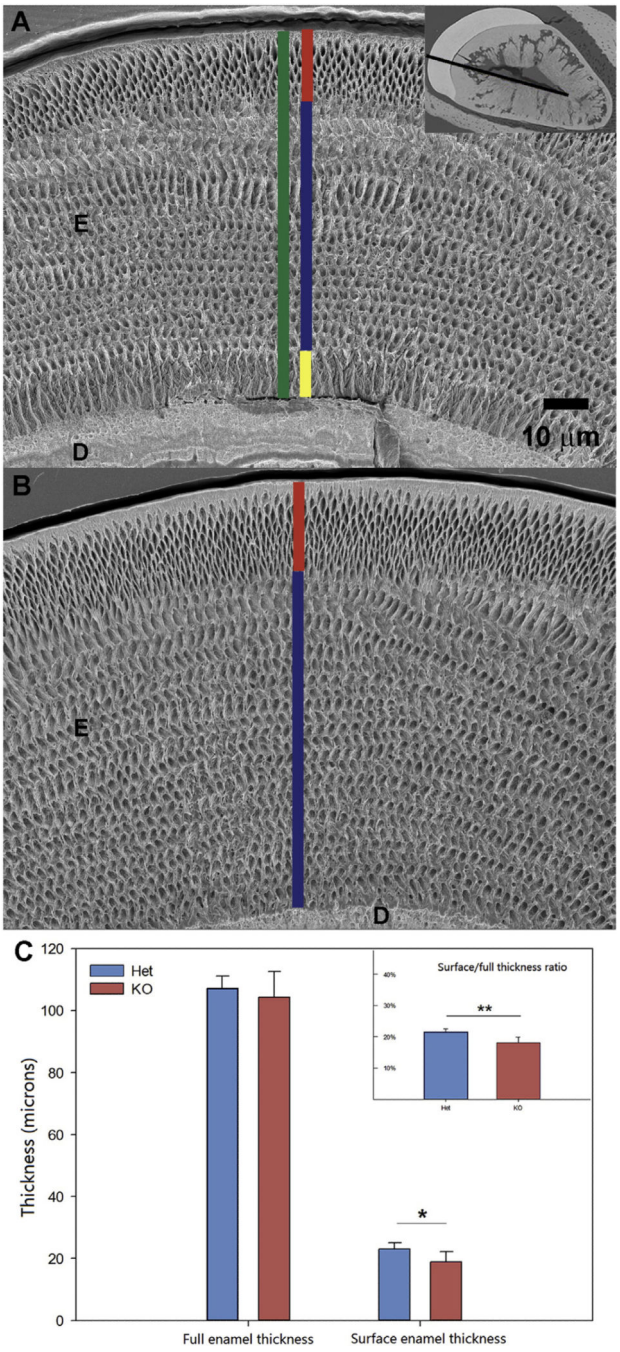

Fig. 5.

The surface thickness of Dspp$^{-/-}$ enamel is similar to Dspp$^{+/-}$, while the total enamel thickness is similar in both genotypes. Measurements of enamel thickness erupted portions of incisors in *Dspp*$^{+/-}$ and *Dspp*$^{-/-}$ one-month-old mice. **A**. SEM micrograph of the *Dspp*$^{-/-}$ erupted incisor showing total enamel thickness in green, surface enamel thickness in red, bulk enamel thickness in blue and inner enamel thickness in yellow. The inset shows the line along which the measurements were carried out, connecting labial and lingual corners of the pulp cavity; **B**. SEM micrograph of the *Dspp*$^{+/-}$ erupted incisor with the bulk enamel

thickness shown in blue and the surface enamel thickness in yellow; **C**. The histograms show total enamel thickness, outer enamel thickness and outer to total enamel thickness ratio. One asterisk identifies $p < 0.05$, two asterisks identify $p < 0.01$. D—dentin, E—enamel. (For interpretation of the references to color in this figure legend, the reader is referred to the web version of this article.)

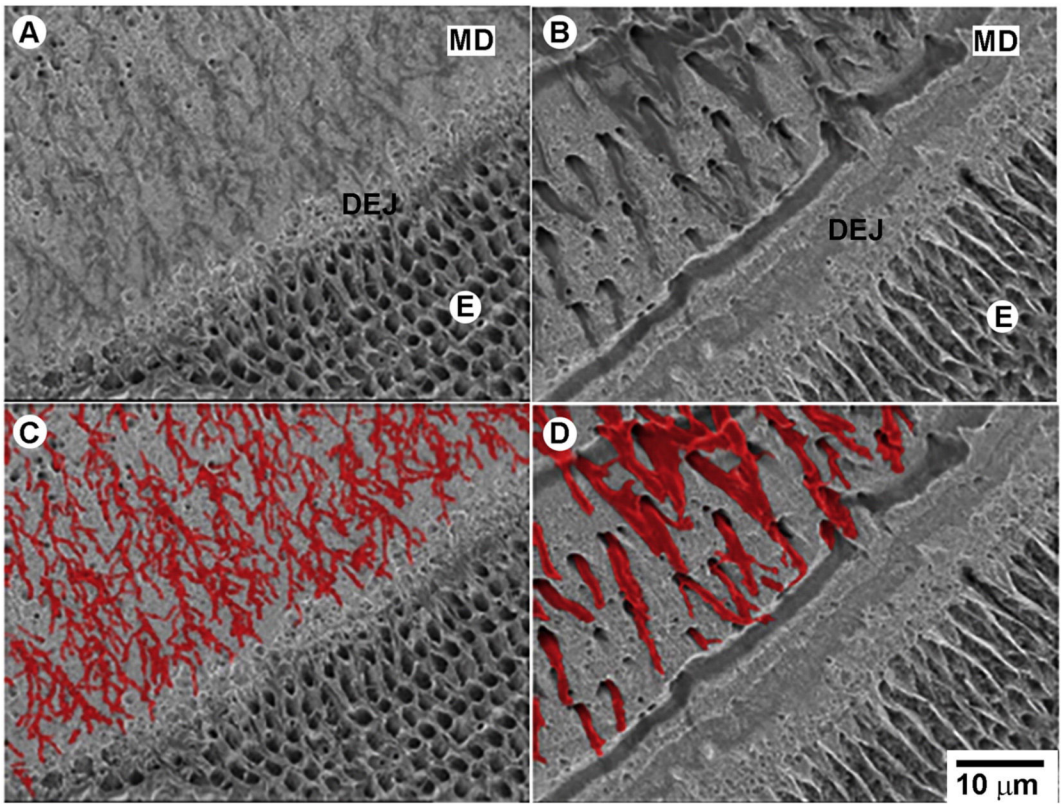

Fig. 6.

Dspp$^{-/-}$ teeth present with major defects at the DEJ, mantle dentin and inner enamel. BS SEM images of etched erupted portions of incisors mice, polished in the transverse plane and resin cast, from one-month-old mice. **A**. *Dspp*$^{+/+}$ and **B**. *Dspp*$^{-/-}$. **C** and **D** correspond to images **A** and **B** with the odontoblasts processes colored for a better visual perception. All micrographs are taken at the same magnification. E—enamel, MD—mantle dentin. (For interpretation of the references to color in this figure legend, the reader is referred to the web version of this article.)

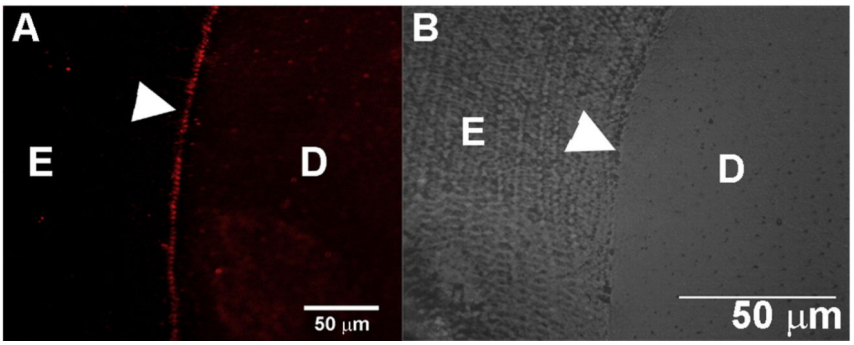

Fig. 7.

DSP protein is present in the DEJ. Immunofluorescence image of a fully mineralized polished section of an erupted mouse incisor showing expression of DSPP. D—dentin, E—enamel.

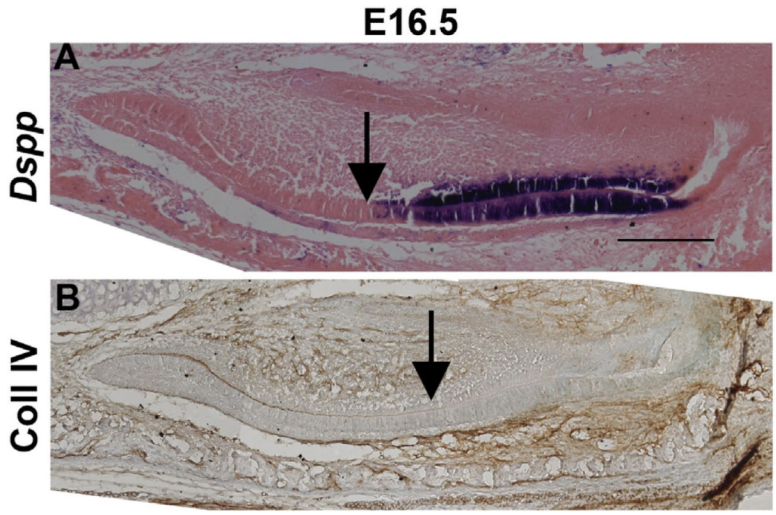

Fig. 8.

Dspp mRNA is expressed in the secretory ameloblasts **A)** (mRNA) *Dspp* expression (purple) is found in the ameloblast and odontoblast layers of the incisor at E16.5. Arrow points to the onset of the DSPP expression. **B)** Collagen IV (brown stain) is found in the basal lamina which is digested during the onset of the secretory stage of amelogenesis (indicated by the arrow). Scale bars = 200 μm.

Table 1

Relative changes in the enamel mineral density and volume.

Enamel stage	Early mid-secretory		Late secretory		Maturation		Mature
Distance from onset of enamel mineralization	0.6–0.8	1.4–1.6	1.6–1.8	1.8–2.0	2–3mm	3–4mm	4–8mm
Mineral density[a]	NS	11%*	19%**	22%**	25%**	14%*	NS
Volume[a]	28%*	NS	−18%*	−17%**	−19%**	−10%**	−13%**

NS — not statistically significant.

[a]% difference between *Dspp*$^{-/-}$/*Dspp*$^{+/-}$.

*p < 0.05.

**p < 0.01.

Table 2

Onset of DSPP mRNA expression in the developing tooth.

	E15.5		E16.5		E17.5		E18.5		P10	
Tooth	**Molar**	**Incisor**	**Molar**	**Incisor**	**Molar**	**Incisor**	**Molar**	**Incisor**	**Molar**	**Incisor**
Odontoblast	–	–	–	+	–	+	++	++	+	+
Ameloblast	–	–	–	+	–	+	++	++	+	+